Phase Behavior of Polylactides in Solvent–Nonsolvent Mixtures

P. VAN DE WITTE,† P. J. DIJKSTRA, J. W. A. VAN DEN BERG, and J. FEIJEN*

Department of Chemical Technology and Institute for Biomedical Technology, University of Twente, P.O. Box 217, 7500 AE Enschede, the Netherlands

SYNOPSIS

Isothermal phase diagrams for the semicrystalline poly-L-lactide (PLLA) and the amorphous poly-DL-lactide (PDLLA) in combination with several solvent–nonsolvent combinations (dioxane/water, dioxane/methanol, chloroform/methanol, and NMP/water) have been determined. The locations of the liquid–liquid miscibility gap, the solid–liquid miscibility gap and the vitrification boundary in the isothermal phase diagrams at 25°C were identified. The liquid–liquid miscibility gap for the systems with PLLA was located in the same composition range as the corresponding systems with PDLLA. For the systems containing PLLA solid–liquid demixing was thermodynamically preferred over liquid–liquid demixing. Attempts were made to correlate the experimental findings with predictions on the basis of the Flory–Huggins theory for ternary solutions using interaction parameters derived from independent experiments. Qualitative agreement was found between the theoretical predictions and the experimentally obtained liquid–liquid miscibility gap. No good agreement was found for the solid–liquid miscibility gap. © 1996 John Wiley & Sons, Inc.

Keywords: ternary phase diagrams • polylactides • Flory–Huggins • demixing • membranes

INTRODUCTION

Membrane formation by immersion of a polymer solution in a nonsolvent has become an important technique for the preparation of porous structures.[1] Phase transitions in solution are responsible for the pore generation and for the fixation of the porous morphology. The commonly observed cellular morphology is due to liquid–liquid demixing by nucleation and growth of a polymer poor phase. The phase-separated structure in the solution can be stabilized by a glass transition or by associations between the components in solution.[2–4] For rapidly crystallizing polymers, also solid–liquid demixing processes can play an important role in the structure formation.[5–7]

Phase diagrams can provide valuable information on the importance of the various phase transitions for a specific membrane forming system. Experimentally obtained liquid–liquid miscibility gaps for cellulose acetate, polysulfone, polystyrene, and polyurethane in several solvent–nonsolvent mixtures have been published in the literature.[8–18] Other phase boundaries like vitrification boundaries or melting and crystallization transitions have been determined for a few ternary systems.[19–24] Occasionally, unknown phase boundaries could not be obtained experimentally, but had to be calculated using parameters extracted from other, experimentally better accessible, phase diagrams. In such cases, usually the Flory–Huggins theory for ternary systems is applied.[16,20,21,23,24]

It is not clear, however, to what extent such phase boundaries, calculated using fits to other phase boundaries, correspond to real (i.e., experimentally determinable) phase boundaries. Cheng et al. claimed that the liquid–liquid miscibility gap calculated with interaction parameters derived from the solid–liquid miscibility gap coincided with the liquid–liquid miscibility gap determined for amorphous nylon.[19] No quantitative agreement, however, was obtained by Burghardt, nor by Altena,

* To whom correspondence should be addressed.
† Currently: Philips Research Laboratories, Prof. Holstlaan 4, 5656 AA Eindhoven, The Netherlands.

Journal of Polymer Science: Part B: Polymer Physics, Vol. 34, 2553–2568 (1996)
© 1996 John Wiley & Sons, Inc. CCC 0887-6266/96/152553-16

although experimental trends were predicted qualitatively.[16,21-24] Moreover, a disadvantage of these studies is that the input parameters of the equations were not derived from other measurements than phase boundary determinations. In addition, a systematic thermodynamic study on the phase behavior of semicrystalline polymer–solvent–nonsolvent systems is still lacking.

This study will address the problems just mentioned in some detail, through comparing experiments and theory for the phase behavior of both semicrystalline poly-L-lactide (PLLA) and amorphous poly-DL-lactide (PDLLA) in several solvent/nonsolvent mixtures (from these polymers, membranes for biomedical purposes can be prepared[6]). The solvent–nonsolvent combinations used for the experiments are: dioxane–water, *N*-methyl pyrrolidone (NMP)-water, chloroform–methanol, and dioxane–methanol. For these eight ternary systems attempts have been made to determine the liquid–liquid miscibility gap, the solid–liquid miscibility gap, and the vitrification boundary. The simple version of the Flory–Huggins theory for ternary solutions, as applied usually (see above), is used first, in order to find out whether this theory indeed can give predictions with respect to the influence of thermodynamic parameters on the phase boundaries in experimental phase diagrams. The thermodynamic input parameters were derived from independent experiments. In an accompanying report, the correlation between phase diagrams and membrane morphologies will be analyzed.

THEORY

The solid–liquid miscibility gap and the liquid–liquid miscibility gap can be calculated using the Flory–Huggins theory for ternary solutions.[25,26] The investigated systems consist of a polydisperse polymer, a solvent, and a nonsolvent. In principle this requires the application of complicated thermodynamical descriptions for multicomponent systems.[27] However, usually the effects of polydispersity are relatively small for ternary solutions of high molecular weight polymers compared to the influence of the interaction parameters.[27] The systems studied here will be considered as quasiternary solutions consisting of a monodisperse polymer, a solvent and a nonsolvent. A thermodynamically exact formulation for ternary polymer solutions has been proposed by Pouchly et al.[28]:

$$\frac{\Delta G_M}{RT} = n_1 \ln \phi_1 + n_2 \ln \phi_2 + n_3 \ln \phi_3 + g_{12} n_1 \phi_2 + g_{13} n_1 \phi_3 + g_{23} n_2 \phi_3 + g_T n_1 \phi_2 \phi_3 \quad (1)$$

ΔG_M = free energy of mixing, n_i represents the number of moles of component i (i = 1: nonsolvent; i = 2: solvent; i = 3: polymer). ϕ_i represents the volume fraction of component i and the g_{ij}-parameters represent the binary interaction parameters between the components i and j. g_T is a ternary interaction parameter and can be regarded as an empirical correction parameter. All interaction parameters g_{ij} can depend on the ratio ϕ_i/ϕ_j, g_T is known to depend on both ϕ_1/ϕ_2 and ϕ_3.[29] The complete determination of all these parameters is a formidable task and has not been attempted up to now. Especially the ternary interaction parameter is poorly accessable and is seldom studied. The thermodynamics of ternary systems often can be approximated with reasonable accuracy without taking this parameter into account.[15-17,19] In a first approximation the parameter will be neglected in the present study. For simplicity, also the concentration dependence of g_{13} and g_{23} will be neglected.

From eq. (1) relations can be derived that describe the liquid–liquid equilibrium and the solid–liquid equilibrium. The chemical potentials ($\Delta\mu$) of the three components are given by the following relations:

$$\frac{\Delta\mu_1}{RT} = \ln \phi_1 + 1 - \phi_1 - s\phi_2 - r\phi_3 + (g_{12}\phi_2 + \chi_{13}\phi_3)(\phi_2 + \phi_3) - s\chi_{23}\phi_2\phi_3 - \phi_2 u_2 (1 - u_2) \frac{dg_{12}}{du_2} + \chi_T \phi_2 \phi_3 (1 - 2\phi_1) \quad (2A)$$

$$\frac{s\Delta\mu_2}{RT} = s \ln \phi_2 + s - \phi_1 - s\phi_2 - r\phi_3 + (g_{12}\phi_1 + s\chi_{23}\phi_3)(\phi_1 + \phi_3) - \chi_{13}\phi_1\phi_3 + \phi_1 u_2 (1 - u_2) \frac{dg_{12}}{du_2} + \chi_T \phi_1 \phi_3 (1 - 2\phi_2) \quad (2B)$$

$$\frac{r\Delta\mu_3}{RT} = r \ln \phi_3 + r - \phi_1 - s\phi_2 - r\phi_3 + (\chi_{13}\phi_1 + s\chi_{23}\phi_2)(\phi_1 + \phi_2) - g_{12}\phi_1\phi_2 + \chi_T \phi_1 \phi_2 (1 - 2\phi_3) \quad (2C)$$

Procedures for calculation of binodals and spinodals have been described by Tompa, by Altena and Smolders, and by Yilmaz and McHugh.[25,26,30]

For our calculations, we preferred the recent computational method presented by Yilmaz and McHugh.[30]

The equation for the melting point depression of a polymer in a solvent/nonsolvent mixture can be derived in an analogous way as for binary solutions, resulting in[19,21,23,31]:

$$\frac{1}{T_m} - \frac{1}{T_m^0} = -\frac{R}{\Delta H_m^0}\frac{v_u}{v_1}\{r \ln \phi_3 + r(1-\phi_3) - \phi_1 - s\phi_2 + (\chi_{13}\phi_1 + s\chi_{23}\phi_2)(\phi_1 + \phi_2) - g_{12}\phi_1\phi_2 + \chi_T\phi_1\phi_2(1-2\phi_3)\} \quad (3)$$

In eqs. (2) through (3) g_T, g_{13}, and g_{23} are assumed to be independent of the polymer concentration, thus $g_{i3} = \chi_{i3}$ and $g_T = \chi_T$. T_m and T_m^0 are the melting temperature of the polymer in solution and the equilibrium melting temperature of the polymer, respectively. g_{12} depends on the composition of the solvent/nonsolvent part of the ternary mixture u_1, u_1 is defined as $\phi_1/(\phi_1 + \phi_2)$. v_u indicates the molar volume of a repeat unit of the polymer and ΔH_m^0 is the heat of fusion for 100% crystalline polymer at the equilibrium melting temperature. $s = v_1/v_2$ and $r = v_1/v_3$, v_i = molar volume of component i.

The variables that represent the properties of the semicrystalline polymer can be grouped into a dimensionless parameter A. A is a measure for the thermodynamic driving force for crystallization of the polymer:

$$A = -\left(\frac{1}{T_m} - \frac{1}{T_m^0}\right)\left(\frac{\Delta H_m^0}{R}\right)\left(\frac{v_1}{v_u}\right) \quad (4)$$

In the derivation of eq. (4) several assumptions have been made.[32] An important one is, that the heat of fusion and the entropy of fusion do not depend on temperature. For large differences in T_m and T_m^0 this assumption is not justified anymore.[32-34] The free energy change, ΔG_m, involved in the melting transition at temperature T is:

$$\Delta G_m^T = \Delta H_m^T - T\Delta S_m^T \quad (5)$$

If the heat capacity difference (ΔC_p) between the melt and the crystalline state is described by $\Delta C_p = D + ET$, the next equation can be derived:

$$A_{Cp} = \left\{\left(\frac{1}{T_m} - \frac{1}{T_m^0}\right)(\Delta H_m^0 - DT_m^0) - \frac{1}{2}E\frac{(T_m^0 - T_m)^2}{T_m} - D\ln\left(\frac{T_m}{T_m^0}\right)\right\}\left(\frac{-v_1}{Rv_u}\right) \quad (6)$$

This procedure was followed earlier by Cheng et al. However their equations, as published, contain several errors.[19] Moreover, their equation does not reduce to Flory's equation for the melting point depression in binary solutions at the polymer–solvent axis and the polymer–nonsolvent axis.[31]

It is interesting to compare the results obtained with the original eq. (4) and the modified eq. (6). The difference between the equations has been analyzed using parameters valid for poly-L-lactide (see later sections). The melting point depression of a polymer in a single solvent was calculated for varying values for the heat of fusion and polymer–solvent interaction parameter neglecting a temperature dependence of the latter. The results are shown in Figure 1.

In Figure 1A the effect of the value of the heat of fusion on the solubility curve is presented. It is clear that this parameter has an enormous impact on the melting transition. A low value for the heat of fusion results in a rapid drop of the melting temperature with the solvent concentration of the solution. For a low heat of fusion the effect of introducing a temperature-dependent heat of fusion and entropy of fusion is considerable. Especially at low polymer concentrations the melting point depression is much stronger when this effect is taken into account. In general, because the heat of fusion and the heat capacities are to some extent related, the magnitude of the effect of introducing a temperature dependence of ΔS_m and ΔH_m will be similar for all polymer–solvent systems.[34] This feature is also predicted by the simplified equation for A as proposed by Hoffman.[33] The polymer–solvent interaction has also a large influence on the solubility curves (Fig. 1B). The effect of introducing a temperature dependence of ΔS_m and ΔH_m is similar for different values for the polymer–solvent interaction parameter.

Interaction Parameters

The input parameters that feature in the equations are the molar volumes and binary interaction parameters. For a useful analysis the interaction parameters have to be determined from independent measurements. The *solvent/nonsolvent interaction parameters* (g_{12}) were derived from literature data on the excess Gibbs energy of mixing (ΔG^E).[29] The *polymer/solvent interaction parameters* χ_{23} were derived from the osmotic pressure (π) using the equation of Flory and Daoust.[35] The *polymer/nonsolvent interaction parameter* χ_{13} is difficult to determine because of the insolubility of the polymer in the

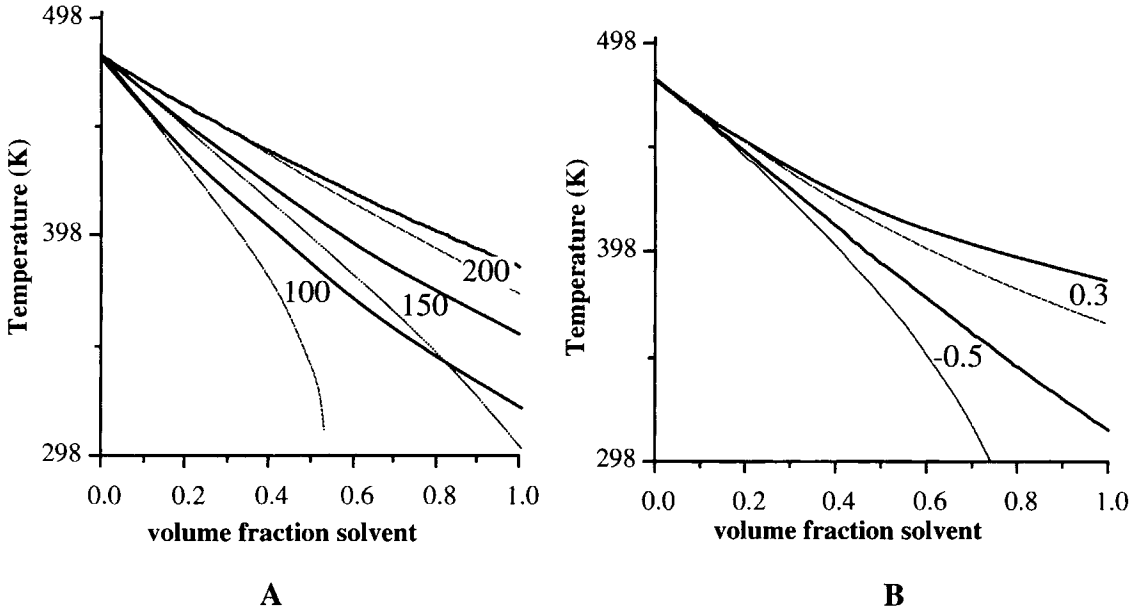

Figure 1. Comparison of two expressions [eq. (4) and eq. (6)] for the driving force for crystallization. Melting point depressions are calculated by neglecting the logarithmic term in eq. (3) (implying a high molecular weight of the polymer). The thin curve of the pair of curves calculated for a set of parameters is based on A_{Cp}, the thick curve is based on A. (A) Influence of the value for the heat of fusion (in J/g) on the solubility curve ($\chi_{23} = 0$). (B) Influence of the value of the polymer–solvent interaction parameter on the solubility curve (heat of fusion 140 J/g). All other parameters apply to the PLLA-chloroform system (see Tables I and II).

nonsolvent. Here the interaction parameter is calculated from the swelling values of the polymer in the nonsolvent.[12]

EXPERIMENTAL

Materials

The PLLA and PDLLA samples were purchased from Purac Biochem (Gorinchem, the Netherlands) or synthesized according to standard procedures.[36] The polymers were purified by dissolving the polymer in chloroform and subsequent precipitation of the solution in methanol. Chloroform was of spectroscopic quality (Lichrosolv, Merck, Darmstadt, Germany). All other solvents were of analytic quality and were purchased from Merck.

Methods

Intrinsic Viscosities

Intrinsic viscosities were determined using an Ubbelohde viscometer at 25.0°C in chloroform. The extrapolation to zero concentration was carried out using a combined Kraemer/Huggins extrapolation. Intrinsic viscosities in the solvent/nonsolvent mixtures were measured using the same procedures. Molecular weights can be calculated according to the following equations: PLLA: $[\eta] = 2.48 \times 10^{-4} M_v^{0.77}$, PDLLA: $[\eta] = 1.33 \times 10^{-4} M_v^{0.79}$ ($[\eta]$ in dL/g, chloroform, 25°C).[37]

Optical Rotation

The optical rotation of PLLA in solvent/nonsolvent mixtures was determined using a Perkin–Elmer 241 polarimeter (25°C). The polymer concentration was 1% w/v. The wave lengths (λ) were: 365 nm, 436 nm, 546 nm, 578 nm, and 589 nm. The intrinsic viscosity of the PLLA sample used was 4.7 dL/g (chloroform, 25°C).

Osmotic Pressure Measurements

Osmotic pressures were measured using a Gonotek-090 osmometer. Membranes were purchased from Schleicher & Schuell (RC53, pore diameter: 0.02 μm, molecular weight cut off: 20 kg/mol) and equilibrated to the solvents used, using solvent gradients.

Swelling Values

Thin films (300 μm) were obtained by solution casting from chloroform, followed by extraction with methanol and extensive drying (three days in vacuo at 85°C). Swelling values were determined by equilibrating thin films in the nonsolvent for several days until a constant weight was attained.

Melting Points and Cloud Points

Polymer, solvent, and nonsolvent were weighed into glass tubes. The tubes were frozen in liquid nitrogen and sealed in vacuo with a flame. For melting point determination the glass tubes were clamped in a rotating wheel and homogenized in a thermostated bath at 80°C. The solutions were subsequently quenched to room temperature and aged for 1 day. Subsequently the phase-separated solutions were reheated at a heating rate of 0.1°C/min. Melting points were determined visually. Cloud points were obtained in a similar way by slowly cooling homogenized polymer solutions (cooling rate 0.1°C/min.). The onset of turbidity was detected using laser light transmission detection. The intrinsic viscosities of the polylactide fractions used for cloud points were 2 dL/g. Due to the very high viscosities of the concentrated polymer solutions the same molecular weight fraction could not be used for the melting point depression measurements. The intrinsic viscosity of PLLA used for the melting points of the gels was 0.7 dL/g. In general it can be stated that the influence of the molecular weight on the solubility curve is negligible. The melting point of this PLLA sample was determined by DSC. A sample was heated from 30 to 150°C at a heating rate of 10°C/min. and from 150 to 200°C at a heating rate of 1°C/min. (Perkin Elmer DSC7). The melting point was taken as the end point of the melting endotherm.

X-Ray Diffraction

Isotropic films (0.5 mm thickness) of PLLA were obtained by solution casting. Diffractograms were recorded at ambient temperature using a Guinier–Simon camera with monochromatic CuK_{α}-radiation.

RESULTS

The Conformation of PLLA and PDLLA in Solvent/Nonsolvent Mixtures

Leenslag and co-workers postulated that PLLA can undergo a conformational change from a random coil conformation to an interrupted helix in chloroform/toluene mixtures.[38] The conformational transition was deduced from sudden increases in the curves for the intrinsic viscosity and the optical rotation of PLLA in the solvent mixture above a certain toluene/chloroform ratio.

The occurrence of coil-helix transitions would complicate the phase behavior of the ternary systems used in this study. Two solvent/nonsolvent combinations have been analyzed for this transition: chloroform/methanol and dioxane/water. The intrinsic viscosity for both PLLA and PDLLA as a function of composition of the solvent/nonsolvent mixture is shown in Figure 2. The PLLA solutions with the highest amount of nonsolvent were close to the solubility limit of PLLA and precipitated after prolonged aging.

No evidence can be found for abrupt changes in coil dimensions. The behavior of PLLA and PDLLA in both solvent/nonsolvent mixtures is similar. Also the optical rotation of PLLA as a function of the nonsolvent concentration in the solvent mixtures dioxane/water and chloroform/methanol does not give indications for conformational transitions at all wave lengths investigated (see Fig. 3 for λ = 589 nm).

Phase Transitions

Cloud Points and Melting Points

For all ternary systems cloud points have been determined. Cloud point temperatures represent the temperature at which homogeneous solutions become turbid during cooling. For solutions with

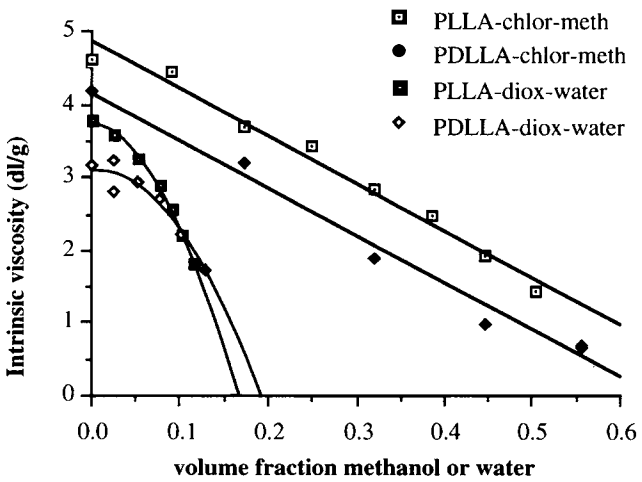

Figure 2. Intrinsic viscosity of PLLA and PDLLA in chloroform/methanol and dioxane/water mixtures. Lines are obtained by linear or quadratic least-squares regression.

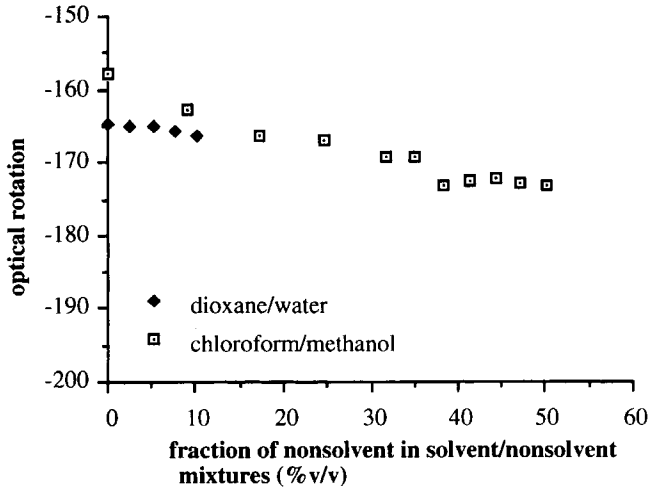

Figure 3. Optical rotation of PLLA in chloroform/methanol mixtures (λ = 589 nm, T = 25°C).

PDLLA the turbidity is induced by liquid–liquid demixing. For solutions with PLLA the turbidity can be induced by crystallization processes or by liquid-liquid demixing processes.

For PLLA-containing solutions also melting points have been determined for solutions with compositions outside the liquid–liquid miscibility gap. To obtain melting points homogenized solutions were quenched to room temperature and reheated after aging for 24 h.

The mechanisms responsible for the onset of turbidity during cooling of ternary polymer solutions can easily be distinguished by recognizing the differences in the rates of phase separation.[13,39] Liquid–liquid demixing results in an almost instantaneous turbidity of the solutions while crystallization processes result in a slow whitening of the polymer solutions. Solutions of the amorphous PDLLA in solvent/nonsolvent mixtures with sufficiently high nonsolvent concentrations turned turbid very rapidly after passing the cloud point temperature indicating that the turbidity is induced by liquid–liquid demixing processes. The solutions became homogeneous again after reheating above the cloud point temperature. After longer equilibration times of phase separated solutions the solutions phase separated completely into two transparent liquid phases.

Solutions with low concentrations of PLLA in dioxane/water mixtures and chloroform/methanol mixtures became turbid rapidly after passing the cloud point temperature in contrast to solutions with low concentrations of PLLA in dioxane/methanol (<10% v/v). Apparently the cloud points obtained for this composition range for PLLA-dioxane–water and PLLA-chloroform–methanol can be attributed to liquid–liquid demixing. In contrast with PDLLA containing solutions PLLA solutions separated into a white solid gel phase and a liquid phase. For more concentrated PLLA solutions in dioxane/water and chloroform/methanol and for all polymer concentrations for the system PLLA-dioxane–methanol and PLLA-NMP-water the phase separation proceeded slowly. This indicates that the cloud points can be attributed to solid–liquid demixing. For PLLA containing solutions large differences were found between the temperature of homogenization and the cloud point temperature.

The importance of the two-phase transitions during membrane formation can be assessed by plotting the cloud points at 25°C in ternary phase diagrams. For all polymer–solvent–nonsolvent systems cloud point temperatures and melting temperatures were measured as a function of polymer concentration and solvent/nonsolvent ratio. A collection of cloud points for PDLLA in dioxane/water mixtures is presented in Figure 4. By extrapolation and interpolation the cloud point compositions at 25°C can be obtained.

Compositions of solutions melting at a certain temperature can be determined in a similar way and can be used for the construction of solubility curves. Compositions melting at 50°C can be determined easily by interpolation. Melting points close to room temperature cannot be obtained because the driving force for crystallization close to the melting point is very low. Therefore solubility curves at 25°C had to be determined by extrapolation and are slightly less accurate.

To allow a better comparison of all systems volume fractions are more suitable than weight frac-

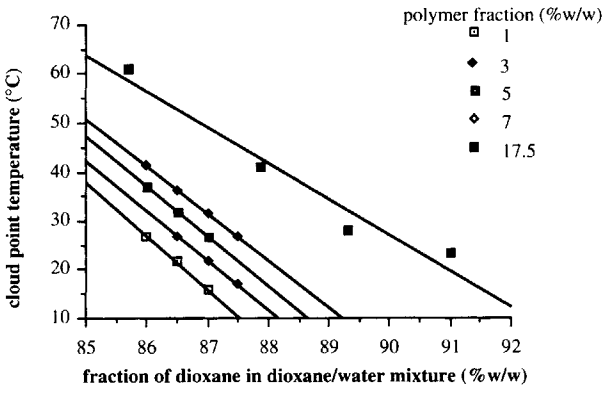

Figure 4. Cloud points for the system PDLLA-dioxane–water. The cloud points are given as a function of dioxane contents of the solvent/nonsolvent mixture for various polymer concentrations.

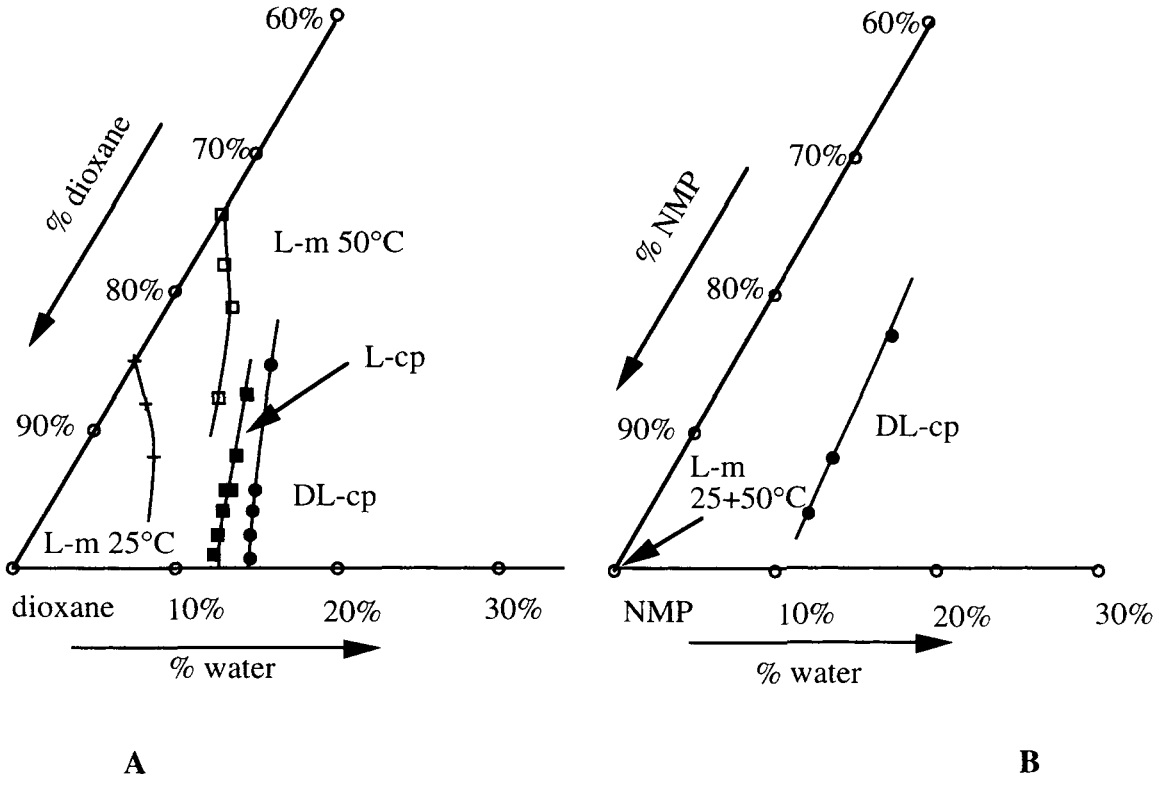

Figure 5. Enlarged isothermal ternary phase diagrams for PLLA-dioxane–water (A), PDLLA-dioxane–water (A), PLLA-NMP-water (B), and PDLLA-NMP-water (B). Abbreviations: L: PLLA, DL: PDLLA, m: solubility curve, cp: cloud point curve at 25°C. Solubility curves are shown for two temperatures (25 and 50°C).

tions. The weight percentages have been converted to volume percentages using the following values for the density: NMP: 1.03 g/cm^3; dioxane: 1.03 g/cm^3; chloroform: 1.48 g/cm^3; water: 1.00 g/cm^3; methanol: 0.79 g/cm^3; PLA: 1.25 g/cm^3.[40,41] The phase diagrams, thus constructed, for the various polymer–

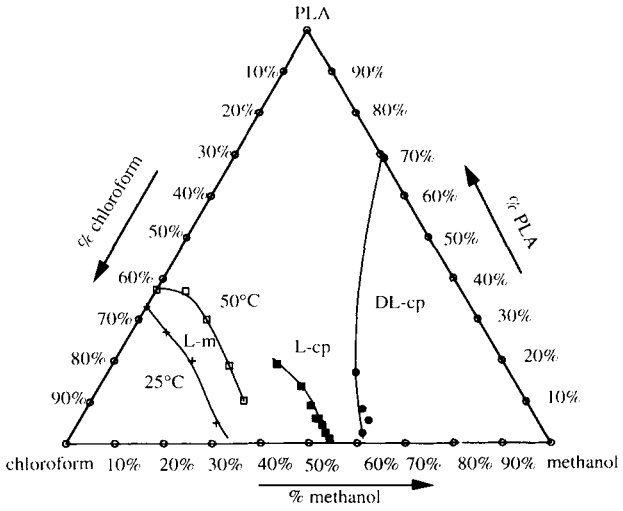

Figure 6. Isothermal ternary phase diagrams for poly-L-lactide and poly-DL-lactide–chloroform–methanol. For abbreviations, see legend Fig. 5.

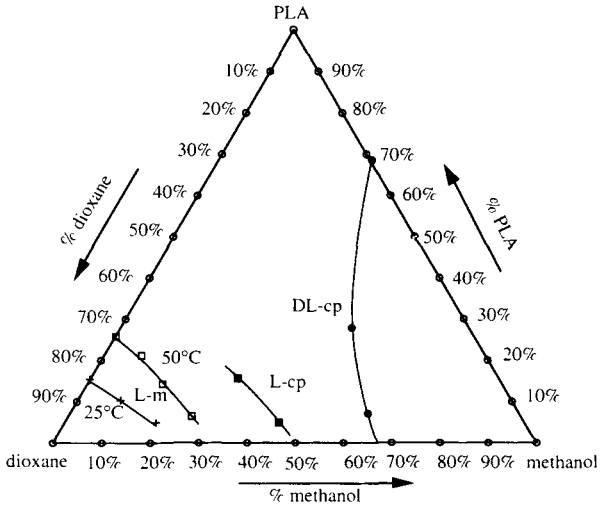

Figure 7. Isothermal ternary phase diagrams for poly-L-lactide and poly-DL-lactide–dioxane–methanol. For abbreviations, see legend Fig. 5.

solvent/nonsolvent systems are shown in Figures 5, 6, and 7.

It is clear that only very small amounts of water are necessary to induce liquid–liquid demixing of PDLLA solutions in dioxane. The differences in location of the cloud point curves between PLLA and PDLLA are small. As already stated above both the cloud point curves for PLLA-dioxane–water and PDLLA-dioxane–water represent the location of the liquid–liquid miscibility gap. The solubility curve is located at lower nonsolvent concentrations than the liquid–liquid miscibility gap.

For PLLA-NMP-water no accurate cloud point curve could be determined due to crystallization of the polymer at the glass wall. At room temperature PLLA already crystallizes from very dilute solutions in NMP. The solubility curve is located at polymer concentrations lower than 1% v/v. The cloud point curve for the system PDLLA-NMP-water is located at slightly lower water concentrations than the corresponding system with dioxane.

The cloud point curves at 25°C for the systems PLLA-chloroform–methanol and PDLLA-chloroform–methanol are shown in Figure 6. The cloud point curve for the system PDLLA-chloroform–methanol is extrapolated to the swelling value at the PDLLA-methanol axis. The cloud point curves are located at much higher nonsolvent concentrations than the cloud point curves for the systems with dioxane and water. The cloud point curves for the systems PDLLA-dioxane–methanol (Fig. 7) and the system PDLLA-chloroform–methanol bend to the nonsolvent axis with increasing polymer concentrations. However, the cloud point curves for the corresponding systems with PLLA gradually bend to the polymer–solvent axis. The part of the cloud point curve for the system PLLA-chloroform–methanol at low polymer concentrations represents the location of the liquid–liquid miscibility gap. At higher polymer concentrations crystallization processes take over (>10% v/v). The curve gradually bends to the polymer–solvent axis. The solubility curve for PLLA again is located at much lower methanol concentrations than the liquid–liquid miscibility gap.

For the system PDLLA-dioxane–methanol similar amounts of methanol are necessary to induce liquid–liquid demixing as necessary for PDLLA-chloroform–methanol. The cloud point curve for the system with PLLA is due to crystallization processes. The distance between the cloud point curve for PLLA and PDLLA is larger than in the case of chloroform/methanol. For PLLA no indications for liquid–liquid demixing were observed. When compared to the system PLLA-chloroform–methanol the solubility curve is shifted to somewhat lower nonsolvent concentrations.

Glass Transition Boundaries

The glass transitions of polylactides with varying amounts of dichloromethane have been measured by Triolo using dynamical mechanical analysis (heating rate 1°C/min., 1 Hz).[42] His data are shown in Fig. 8. From the graph it becomes clear that approximately 7–10% w/w dichloromethane is necessary to decrease the glass transition of PDLLA from 55 to 25°C and 10–12% w/w for PLLA. The value obtained for PLLA is likely to be influenced by the crystallinity of PLLA.

The glass transition depression of the polymer by the solvent depends to a large extent on the glass transition of the solvent. Because the glass transitions for small solvent molecules are usually located in the same temperature range (100–150 K), it is assumed that the glass transition depressions induced by the solvents and nonsolvents used for this study are comparable with those induced by dichloromethane.[43,44]

Interaction Parameters

Solvent/Nonsolvent Interaction Parameters

The interaction parameter for NMP-water is given by Zeman and Tkacik.[12] The interaction parameters for dioxane–methanol, chloroform–methanol and dioxane–water are calculated from excess free energy of mixing data in literature.[45–47] The results are

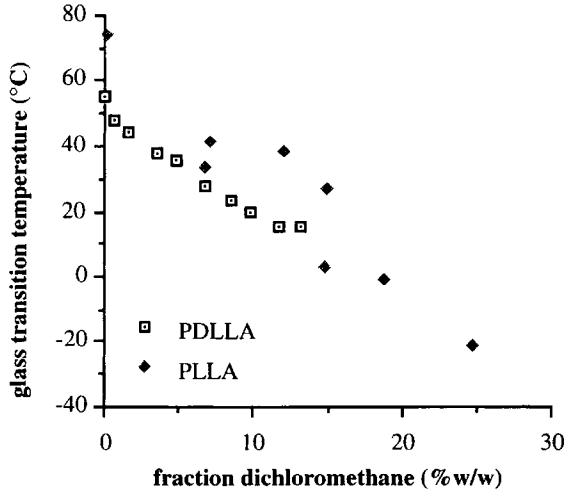

Figure 8. Glass transition of poly-L-lactide and poly-DL-lactide as a function of dichloromethane contents. Reproduced from Triolo.[42]

shown in Figure 9. All values are obtained at 25°C except for the values for chloroform/methanol (35°C) and dioxane/methanol (30°C). Values for the heat of mixing indicate that these interaction parameters do not change much in this small temperature range.[48] For chloroform/methanol and dioxane/water the interaction parameters are strongly composition dependent. Especially at low nonsolvent concentrations the interaction parameters are high, indicating that these solvent/nonsolvent mixtures are far from ideal. At high nonsolvent concentrations the differences between the interaction parameters are rather small. For NMP/water and dioxane/methanol the interaction parameters hardly change with composition.

Polymer–Solvent Interaction Parameters

Polymer–solvent interaction parameters were determined osmometrically for both polymers with chloroform and dioxane. The membranes used (regenerated cellulose) were not suitable for measurements using NMP. The swelling of the membrane in NMP was too high.

The results for dioxane and chloroform are shown in Figure 10. Except for very low polymer concentrations consistent values for the interaction parameters were obtained. At low polymer concentrations the error in the determination of the osomotic pressure is relatively large. In a previous study it was demonstrated that the data obtained for chloroform are in good agreement with interaction parameters derived from a Stockmayer–Fixman analysis of molecular weight determinations.[37] No dependency of the interaction parameter on the polymer concentration can be detected for the examined concentration range. For both chloroform and dioxane PLLA has a somewhat better interaction with the solvent than PDLLA. Chloroform is a better solvent than dioxane for both polymers. An indication for the polymer–solvent interaction can also be obtained from intrinsic viscosity determinations. The intrinsic viscosity of PDLLA in NMP was lower than the intrinsic viscosity in dioxane and chloroform (For one sample, $[\eta]$ = 2.3 dL/g in NMP, 4.2 dL/g in chloroform, 3.2 dL/g in dioxane). This indicates that the interaction parameter of PDLLA with NMP is higher than the interaction parameter of PDLLA with dioxane or chloroform. The intrinsic viscosity measurements confirm that for PLLA and PDLLA chloroform is a better solvent than dioxane (see Fig. 2).

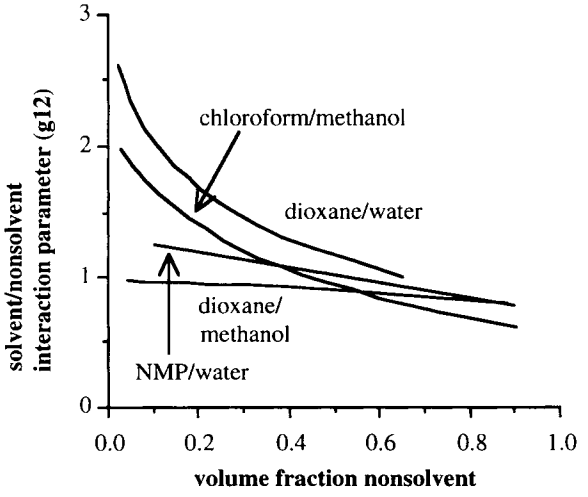

Figure 9. Solvent–nonsolvent interaction parameters as a function of nonsolvent volume fraction.

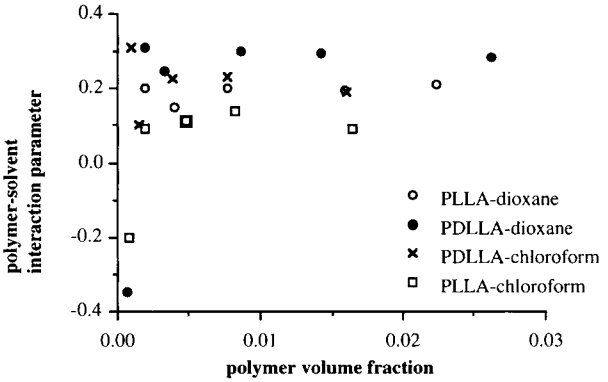

Figure 10. Polymer–solvent interaction parameters as a function of polymer volume fraction. All data were obtained at 25°C.

Polymer–Nonsolvent Interaction Parameters

The equilibrium swelling value of PDLLA in methanol amounts ca. 31 ± 2% v/v. The value calculated for χ_{13} is 1.0. The swelling value of PLLA in methanol was 11 ± 0.5% v/v. Because of the high crystallinity of the PLLA films (estimated crystallinity is 30%) this value cannot be used for the determination of χ. The swelling value for PDLLA in water was approximately 1.4 ± 0.3%. The swelling for PLLA was even lower and could not be determined accurately. The value for χ_{13} calculated for PDLLA is 3.4 ± 0.2.

DISCUSSION

Conformation

The data on the optical rotation and intrinsic viscosities indicate that at least for the systems chlo-

roform/methanol and dioxane/water no abrupt conformational transitions of PLLA occur. The reason why a conformational transition of PLLA is found for chloroform/toluene mixtures[38] and not for dioxane/water and chloroform/methanol may be attributed to the fact that both chloroform and toluene are solvents for PDLLA. PLLA is poorly soluble in toluene because the polymer crystallizes from toluene at room temperature and not because toluene is a thermodynamic nonsolvent (i.e. $\chi > 0.5$) for PLLA. Undoubtedly the solvent quality of toluene for PLLA is lower than that of chloroform. The intrinsic viscosity of PLLA in chloroform/toluene mixtures decreases with increasing toluene concentrations. Probably the interactions between the polymer segments in PLLA/chloroform/toluene solutions are sufficiently strong to allow the formation of longer helical segments. Because of the much higher nonsolvent power of water and methanol the coil-helix transition, if it occurs at all, will be confined to a much smaller composition range than for the chloroform–toluene system.

The intrinsic viscosity of both PLLA and PDLLA in chloroform/methanol mixtures decreases in a similar way with increasing methanol concentrations. For dioxane/water the decrease of the intrinsic viscosity with the percentage of water is somewhat smaller in the case of PDLLA. Despite of the general agreement it cannot be concluded that PLLA and PDLLA possess the same conformation in solution. The unperturbed dimensions of PLLA in chloroform are known to be larger than for PDLLA.[49] Furthermore the interaction of PLLA with the solvents chloroform and dioxane is slightly more favourable than that of PDLLA (see χ_{23} determinations). It can be expected that these differences are at least partly responsible for the small differences in location of the phase boundaries.

When the behavior of the polymers in dioxane/water and chloroform/methanol is compared, it is clear that dioxane is a poorer solvent than chloroform and water is a much more powerful nonsolvent than methanol.

Cloud Point Curves

The large differences in demixing rates between liquid–liquid demixing and solid–liquid demixing processes and the large hysteresis effects involved in solid–liquid demixing can be attributed to the high activation energy necessary for crystallization and the low rates of diffusion of the polymer chains to the growing crystallites. A more detailed analysis of the influence of cooling rates on the phase separation processes occurring in PLLA-chloroform–methanol and PDLLA-chloroform–methanol has been reported elsewhere.[39] For PDLLA apparently no other transition interfered with the liquid–liquid demixing process. The hysteresis effects demonstrate that for PLLA crystallization competed with liquid–liquid demixing. For rapidly demixing solutions of PLLA crystallization occurs in the polymer rich phase after liquid–liquid demixing and for slowly demixing systems demixing occurs predominantly by crystallization.

The differences in location of the liquid–liquid miscibility gap for PLLA and PDLLA appear to be small. The cloud point curve for PLLA is usually located at lower nonsolvent concentrations than for PDLLA. The difference is larger for chloroform–methanol than for dioxane–water. For the systems PLLA-dioxane–methanol and PLLA-NMP-water no indication could be obtained for the location of the liquid–liquid miscibility gap. Small differences in the location of the cloud point curves can result from differences in molecular weight or molecular weight distribution. Since the molecular weight of PDLLA is higher than that for PLLA and both polymers have a similar molecular weight distribution the differences must result from the small differences in interaction parameters. From Figure 10 it becomes clear that small differences in the polymer–solvent interaction parameters exist between PLLA and PDLLA. However, especially small differences in polymer–nonsolvent interaction parameters can be expected to have relatively large effects on the magnitude of the liquid–liquid miscibility gap. Unfortunately this can not be verified for our systems because this parameter cannot be determined accurately.

The location of the cloud point curves and solubility curves for the different solvent–nonsolvent systems differs to a large extent. For the systems with water only a small amount of water is required to induce demixing in the polymer solutions. A much larger amount of methanol is needed to induce liquid–liquid demixing in solutions of polylactides. Trends found for the liquid–liquid miscibility gap are also reflected in the solubility curves. For all systems that were investigated solid–liquid demixing is thermodynamically preferred over liquid–liquid demixing for the entire composition range.

It is interesting to see to what extent the theoretical equations can reproduce the location of the liquid–liquid miscibility gap in the phase diagram. Most of the parameters present in the equations are available. The data are collected in Table I. The polymer–nonsolvent interaction parameter was only

Table I. Values for the Input Parameters in the Equations

Variable	Value	Variable	Value
^{x}PDLLA-dioxane	0.3	^{g}dioxane-methanol	0.9
^{x}PDLLA-chloroform	0.2	^{g}chloroform(2)-methanol(1)	$2.06 - 4.12u_1 + 4.89u_1^2 - 2.33u_1^3$
^{x}PDLLA-water	3.4	r^{b}	0.00085
^{x}PDLLA-methanol	1	v $CHCl_3$	80 cm^3/mol
^{x}PLLA-dioxane	0.2	v methanol	40 cm^3/mol
^{x}PLLA-chloroform	0.1	v dioxane	85 cm^3/mol
^{g}dioxane (2)-water (1)[a]	$1.389 - 0.607u_1 + 1.050\exp(-4.731u_1) + 0.500\exp(-19.922u_1)$	v water	18 cm^3/mol
		v NMP	96 cm^3/mol
^{g}NMP-water	1		

[a] Care has to be taken that good fits of the g_{12} data are obtained in case these parameters strongly depend on composition. Artefacts like miscibility gaps at the solvent-nonsolvent axis are easily generated. The fit of the g_{12} parameter for the dioxane-water mixtures is taken from Reuvers.[17]

[b] This value for r is based on the number average degree of polymerization of PLLA with respect to the molar volume of water. In principle r has to be adjusted for each polymer-nonsolvent combination. However this results in negligible changes in the location of the phase boundaries.

obtained for PDLLA. It is assumed that the polymer–nonsolvent interaction parameter for PLLA is the same as for PDLLA. The calculated curves and the experimental curves for the different polymer–solvent–nonsolvent systems are compared in Figure 11. χ_{13} is only known at high polymer concentrations and is considered to be the least accurate interaction parameter. Therefore for each system the calculated liquid–liquid miscibility gaps are given for several values for χ_{13}. The differences between the calculated liquid–liquid miscibility gaps between PLLA and PDLLA are very small. In the graphs only the curves for PLLA are shown.

It is clear that the experimentally found trends are predicted correctly. However more than qualitative agreement is not obtained. In view of the simplified thermodynamic relations that have been used and the small concentration range used for the determination of the polymer–nonsolvent and the polymer–solvent interaction parameters better agreement may not be expected.

A better fit to the experimental points can be obtained by choosing a lower value for the polymer–nonsolvent interaction parameter. The optimal χ_{13} value for the systems with dioxane–water is 2.5 and for the systems with methanol is 0.9.

Now, we will discuss the correlation between the experimental solubility curve and the theoretical predictions for this curve. The additional parameters that have to be introduced in the formulas are collected in Table I and Table II. For the calculations, the polymer–nonsolvent interaction parameters will be used which resulted in the best fit of the cloud point curves. Some uncertainty exists for the correct value for the heat of fusion. The heat of fusion of 100% crystalline PLLA as estimated by Fischer et al. is 81–93 J/g.[50] Iannace et al. presented a value of 78.6 J/g.[51] However, recent reports have indicated that these values must be too low.[52-54] Loomis et al. suggested, without experimental evidence, that the heat of fusion for PLLA is about 140 J/g.[54] The heat of fusion of racemic crystals of PLLA and PDLA (stereocomplexes) was also determined to be 140 J/g. The value for the stereocomplex was confirmed by Tsuji et al. using x-ray diffraction and NMR.[55] We determined the crystallinity of a solution cast PLLA film by x-ray diffraction. The crystallinity of the film was 26 ± 5%. The heat of fusion of the sample as determined by DSC was 31 ± 1 J/g. The heat of fusion of 100% crystalline PLLA can be calculated to be 120 ± 20 J/g.

Also no extensive heat capacity data are available for PLLA. For the structurally related polyester polyglycolic acid (PGA) the following heat capacity relations are available:[56]

$$C_{p,\text{solid}} = 13.97 + 0.17151T$$

$$C_{p,\text{liquid}} = 100.80 + 0.038092T \qquad (10)$$

$C_{p,\text{solid}}$ represents the heat capacity of the crystalline phase. $C_{p,\text{liquid}}$ represents the heat capacity of the melt. Both relations are in J/mol K. Heat capacity data estimated from group contributions given by Van Krevelen indicate that the heat capacity in J/g is the same for both PGA and PLLA.[34] Therefore, approximate C_p relations for PLLA can be obtained by multiplying the heat capacity rela-

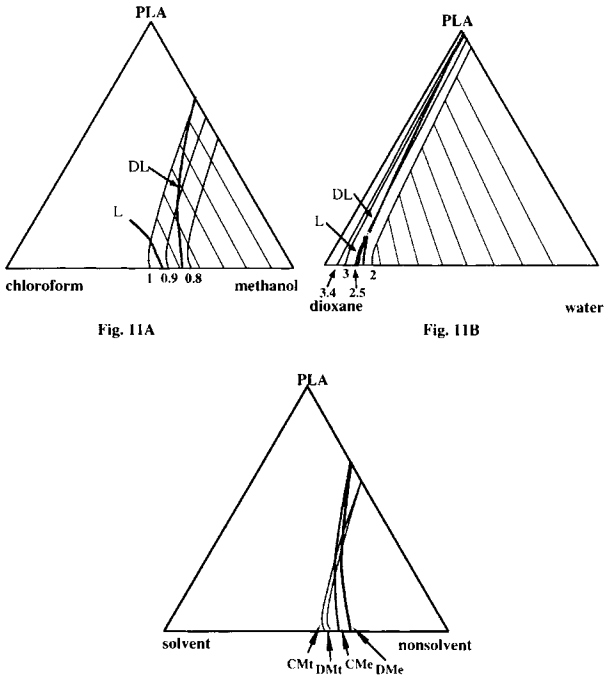

Figure 11. Comparison between theoretically calculated liquid–liquid miscibility gaps and experimentally determined liquid–liquid miscibility gaps. Shaded lines represent experimental cloud point curves. Solid lines represent calculated phase boundaries. In some cases tie lines have been given for a certain set of interaction parameters. Numbers indicate the value of χ_{13} used for the calculations. (A) PLA-chloroform–methanol. (B) PLA-dioxane–water. (C) PDLLA-dioxane–methanol and PDLLA-chloroform–methanol. $\chi_{13} = 0.9$. CMt: theoretical curve for PDLLA-chloroform–methanol, DMt: theoretical curve for PDLLA-dioxane–methanol, CMe: experimental curve for PDLLA-chloroform–methanol, DMe: experimental curve for PDLLA-dioxane–methanol.

tions for PGA by the ratio of the molecular weight of the repeat unit of PLLA and PGA (factor: 72.06/58.04).

Using this set of parameters, the polymer concentration of the solid–liquid transition on the polymer–solvent axis can be calculated. For a heat of fusion of 140 J/g and T_m^0 of 480 K the solubility limit at 25°C in chloroform was calculated to be less than 1%. For agreement with experimental values (33% v/v) a value of 98 J/g had to be taken for the heat of fusion using a T_m^0 of 480 K. A similar heat of fusion is necessary when the actual melting point of the pure PLLA sample is used for the calculations (449 K as determined by DSC). This heat of fusion is somewhat lower than the value obtained from our measurements. We will return to this issue in a later section.

The polymer–solvent interaction parameter is known only at low polymer concentrations. The polymer–solvent interaction parameter influences the polymer concentration at the polymer–solvent axis to a smaller extent. Changes in the values for χ_{23} from 0.1 to 0 or 0.2 shift the polymer concentration to 38% and 27%, respectively. The reported heat of fusion (98 J/g) and T_m^0 (449 K) have also been used for the other systems. The calculated solubility curves are shown in Figure 12.

It is encouraging to note that the lower solubility limit on the PLLA-dioxane axis is predicted correctly. Due to the small molar volume of the nonsolvents, the solubility curve shifts to higher polymer concentrations at increasing nonsolvent concentrations. In the theoretical description the effect of differences in molar volumes of the low molecular weight compounds appears to be overestimated. The solubility curve intersects the liquid–liquid miscibility gap at very high polymer concentrations. This is in contradiction with the melting points and cloud points found experimentally. Experimentally, the polymer concentration of the solubility curve decreases with increasing nonsolvent concentrations. The reason for the discrepancy between the experimental curve and the theoretical curve is unclear but may be attributed to several phenomena.

1. Because much better agreement is obtained for the liquid–liquid miscibility gap, it is likely that the used values for the binary interaction parameters are sufficiently accurate to obtain qualitative agreement for the solubility curve. No improvement in the description can be obtained by small changes in the interaction

Table II. Values for the Input Parameters in the Equations

Variable	Value	Variable	Value
Density PLA[41]	1.25 g/cm^3	T_m^0 PLLA[55]	480 K
Mu_{PLLA}[a]	72.06 g/mol	ΔH_m PLLA	81 − 140 J/g
		$\Delta C_p = D + ET$, PLLA	$107.8 - 0.1656T$

[a] Molecular weight lactic acid repeat unit.

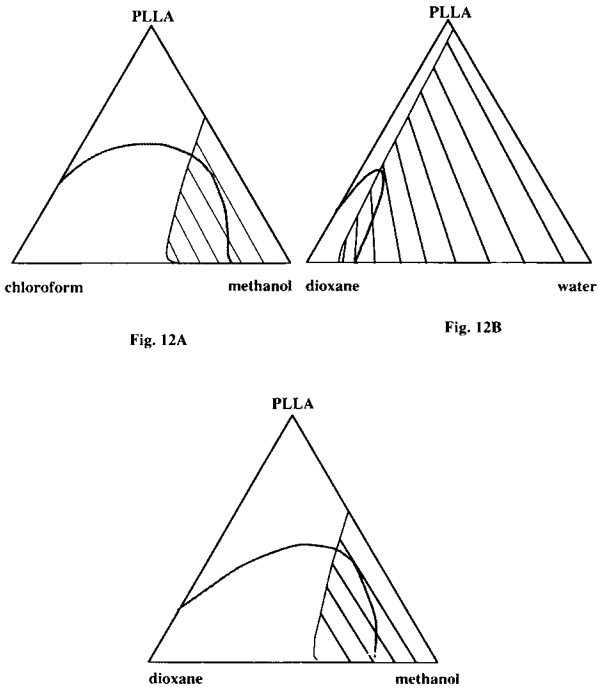

Figure 12. Calculated phase diagrams (25°C) for (A) PLLA-chloroform–methanol, (B) PLLA-dioxane–water, and (C) PLLA-dioxane–methanol.

parameters. However, it cannot be excluded that a ternary interaction parameter is required for an accurate description of the thermodynamics of the system. It is well-known that for an accurate description of the intrinsic viscosity or the preferential sorption of polymers in mixed solvents also ternary interaction parameters are required.[29,57-63] This applies especially to systems like ours: methanol and water are self-associating compounds, and, in addition, hydrogen bonding can occur between the polymers and the nonsolvents, and between the solvents and the nonsolvents. Furthermore, it is known that chloroform specifically interacts with the ester group of polylactides.[49] Thus, we should have incorporated a ternary interaction parameter into our calculations. However, from a preliminary study (see Appendix) it appears that the ternary interaction parameter influences the liquid–liquid miscibility gap to a larger extent than the solid–liquid miscibility gap and thus cannot explain the deviations between theory and experiment.

2. A source for deviations may arise from the nonequilibrium nature of the crystallites. In the derivation of eq. (3) it has been implicitly assumed that no size differences exists between the lamellae of crystallites obtained under different conditions. This is no problem at polymer concentrations higher than 50% but the more dilute the solution the smaller the lamellar thickness will get.[33,64] However, this would give rise to deviations in the opposite directions than found experimentally. Experimentally the polymer concentration at the solubility curve decreases continuously with increasing nonsolvent concentrations. If the lamellar thickness decreases with decreasing polymer concentrations the actual equilibrium solubility curve will shift to even lower polymer concentrations.
3. Another possibility may be that the solvent power of the solvents for PLLA is sufficiently high to enable complex formation between the solvent and the polymer, or inclusion of solvent in the crystal lattice.[65] If this is true, the theoretical descriptions used are indeed oversimplified and inadequate. In this case better descriptions cannot be expected from improved descriptions of ternary polymer solutions but from better descriptions of the chemical potential of the polymer crystals.[65]

The only other way to reconcile the theoretical calculations with the experimental results is to take a higher value for the heat of fusion. To maintain the correct intersection point at the polymer–solvent axis the interaction parameter has to be decreased to very low values. In Figure 13 some heat of fusion/χ_{23} combinations are presented using the parameters for the system PLLA-chloroform–methanol. These variations of the polymer–solvent interaction parameter in the good solvent range (low χ_{23} range) only marginally influence the location of the liquid–liquid miscibility gap but are very important for the solubility curve.

The χ_{23} interaction parameters obtained from osmometry were much higher than those used in Figure 13 for the high heats of fusion. This implies a large concentration dependency of the polymer–solvent interaction parameter. For polymers carrying ester groups in the side chain negative interaction parameters in chloroform are not uncommon.[66]

Nevertheless, it is admitted that the procedure followed for the solubility curve has become rather arbitrary and therefore is not very satisfactory. More experiments have to be performed to clear up these controversies. At the moment it is not known whether these results are limited to our systems or are of general nature. Cheng et al. and Altena et al.

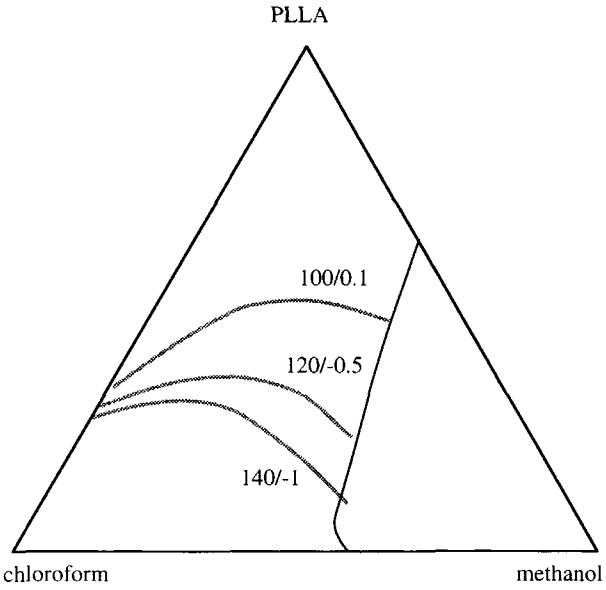

Figure 13. Phase diagrams for the system PLLA-chloroform–methanol calculated for three $\Delta H/\chi_{23}$ combinations. The liquid–liquid miscibility gap is hardly influenced by the indicated changes in the polymer–solvent interaction parameter.

claim to obtain quantitative agreement between theory and experiments.[16,19] However some values for the input parameters (like interaction parameters or heat of fusion) were derived from the experimental solubility curves themselves and the agreement may be fortuitous. In general it can be stated that no reliable values for the interaction parameters can be obtained from melting point depression data.[67] The sensitivity of the results with respect to the input parameters is too large. In view of the earlier discussion on the A-parameter the equations used by these authors are subject to some doubts.

CONCLUSIONS

The solubility curves, the cloud point curves and vitrification boundaries for several polylactide–solvent–nonsolvent systems have been determined. The liquid–liquid miscibility gap for the systems with the semicrystalline PLLA were located in a similar composition range as the corresponding systems with the amorphous PDLLA. For all PLLA-solvent–nonsolvent systems studied solid–liquid demixing was preferred thermodynamically over liquid–liquid demixing. The Flory–Huggins theory for ternary polymer solutions can provide a qualitative indication for the relative locations of the liquid–liquid miscibility gaps. The Flory–Huggins description of the solubility curves was less satisfactory.

SYMBOLS

(i or j = 1: nonsolvent, i or j = 2: solvent, i or j = 3: polymer)

A	dimensionless parameter
C_p	heat capacity (J/mol K)
D, E	constants in the equation for the heat capacity (J/mol K, J/mol K^2)
ΔG_M^T	free energy of fusion (J/mol)
g_{ij}, χ_{ij}	binary interaction parameter between component i and j
g_T	ternary interaction parameter
ΔH_M^T	heat of fusion at temperature T (J/mol)
M_v	viscosity average molecular weight (g/mol)
M_u	molecular weight repeat unit (g/mol)
r	v_1/v_3
s	v_1/v_2
T	temperature (K)
T_m^0	equilibrium melting temperature of the polymer (K)
T_m	melting temperature of the polymer (K)
u_i	$\phi_i/(\phi_1 + \phi_2)$
v_u	molar volume repeat unit of the polymer (cm^3/mol)
v_i	molar volume of the components (cm^3/mol)
ϕ_i	volume fraction of component i
ϕ_3''	polymer volume fraction in the polymer-rich phase
$[\eta]$	intrinsic viscosity (dL/g)

APPENDIX. THE INFLUENCE OF TERNARY INTERACTION PARAMETERS ON THE LOCATION OF THE PHASE BOUNDARIES

The influence of ternary interaction parameters on the location of the phase boundaries cannot be ruled out beforehand. An extensive study of the influence of the ternary interaction parameter χ_T on the location of the liquid–liquid miscibility gap was presented recently by Li in ref. 18. Some examples of the influence of χ_T on both the solid–liquid miscibility gap and the liquid–liquid miscibility gap are presented in Figure A1. In Figure A1A the sensitivity of the location of the phase boundaries for the system PLLA-chloroform–methanol for χ_T is presented. In Figure A1B additional examples for an arbitrarily chosen set of interaction parameters are presented. The results indicate that the influence of

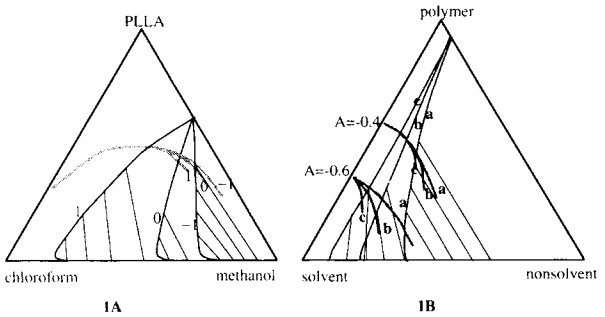

Figure A1. The sensitivity of the location of the phase boundaries towards χ_T. The solubility curves were calculated for an infinitely high molecular weight. The effect of this assumption on the solubility curve is negligible. The solubility curves were extended only partially into the liquid–liquid miscibility gap. (A) Parameters valid for the system PLLA-chloroform–methanol. Indicated numbers represent χ_T. (B) $\chi_{23} = 0.1$; $\chi_{12} = 1$; $\chi_{13} = 1$; $r = 0.0001$; $s = 1$; a: $\chi_T = -1$; b: $\chi_T = 0$, c: $\chi_T = 1$.

χ_T on the liquid–liquid miscibility gap is much larger than the influence on the solid–liquid miscibility gap.

The effects of χ_T on the liquid–liquid miscibility gap are larger than on the solid–liquid miscibility gap. Positive values of χ_T increase the magnitude of the liquid–liquid miscibility gap, negative values of χ_T decrease the magnitude of the liquid–liquid miscibility gap. The influence of χ_T on the solubility curve at high (less negative) A values is negligible. For low values of A positive values for χ_T shift the solubility curve to lower polymer concentrations. The effects of the indicated changes in χ_T on the location of the solubility curve are significant but do not modify the general trends induced by the binary interaction parameters. Because a reasonably good indication for the liquid–liquid miscibility gap was obtained with the neglection of χ_T it is not necessary to include χ_T in the description of the solubility curve.

REFERENCES AND NOTES

1. M. Mulder, *Basic Principles of Membrane Technology,* Kluwer Academic Publishers, Dordrecht, The Netherlands, 1992.
2. J-M. Guenet, *Thermoreversible Gelation of Polymers and Biopolymers,* Academic Press, London 1992.
3. M. J. Miles, *Developments in Crystalline Polymers-2,* D. C. Bassett, Ed., Elsevier Applied Science, New York, 1988, p. 233.
4. J. Arnauts, H. Berghmans, and R. Koningsveld, *Makromol. Chem.,* **194,** 77 (1993).
5. A. M. W. Bulte, B. Folkers, M. H. V. Mulder, and C. A. Smolders, *J. Appl. Polym. Sci.,* **50,** 13 (1993).
6. P. van de Witte, H. Esselbrugge, A. M. P. Peters, P. J. Dijkstra, J. Feijen, R. J. J. Groenewegen, J. Smid, J. Olijslager, J. M. Schakenraad, M. J. D. Eenink, and A. P. Sam, *J. Controlled Release,* **61,** 24 (1993).
7. D. R. Lloyd, K. E. Kinzer, and H. S. Tseng, *J. Membr. Sci.,* **52,** 239 (1990).
8. W. W. Lau, M. D. Guiver, and T. Matsuura, *J. Appl. Polym. Sci.,* **42,** 3215 (1991).
9. B. T. Swinyard and J. A. Barrie, *Br. Polym. J.,* **20,** 317 (1988).
10. Y. S. Kang, H. J. Kim, and U. Y. Kim, *J. Membr. Sci.,* **60,** 233 (1991).
11. M. Mulder, J. Oude Hendrikman, J. G. Wijmans, and C. A. Smolders, *J. Appl. Polym. Sci.,* **30,** 2805 (1985).
12. L. Zeman and G. Tkacik, *J. Membr. Sci.,* **36,** 119 (1988).
13. A. J. Reuvers, F. W. Altena, and C. A. Smolders, *J. Polym. Sci.: Part B,* **24,** 783 (1986).
14. A. Bottino, G. Camera-Roda, G. Capanelli, and S. Munari, *J. Membr. Sci.,* **57,** 1 (1991).
15. L. Utracki, *J. Appl. Polym. Sci.,* **22,** 399 (1962).
16. F. W. Altena, *Phase Separation Phenomena in Cellulose Acetate Solutions in Relation to Asymmetric Membrane Formation,* PhD thesis University of Twente, 1982.
17. A. J. Reuvers, *Membrane Formation,* PhD thesis University of Twente, 1987.
18. S-G. Li, *Preparation of Hollow Fiber Membranes for Gas Separation,* PhD thesis University of Twente, 1994.
19. L. P. Cheng, A. H. Dwan, and C. C. Gryte, *J. of Polym. Sci. Part B: Pol. Phys.,* **32,** 1183 (1994).
20. G. E. Gaides and A. J. McHugh, *Polymer,* **30,** 2118 (1989).
21. F. W. Altena, J. S. Schroder, R. van de Huls, and C. A. Smolders, *J. of Polymer Sci.: Part B,* **24,** 1725 (1986).
22. D. M. Koenhen, M. H. V. Mulder, and C. A. Smolders, *J. of Appl. Polym. Sci.,* **21,** 199 (1977).
23. W. R. Burghardt, L. Yilmaz, and A. J. McHugh, *Polymer,* **28,** 2085 (1987).
24. A. M. W. Bulte, *Nylon 4,6 as Membrane Material,* PhD thesis, University of Twente 1994.
25. H. Tompa, *Polymer Solutions,* Butterworths Scientific Publishers, London 1956.
26. F. W. Altena and C. A. Smolders, Macromolecules, **15,** 1491 (1982).
27. R. Koningsveld, *Chem. Zvesti,* **26,** 263 (1972).
28. J. Pouchly, A. Zivny, and K. Solc, *J. of Polym. Sci. Part C,* **23,** 245 (1968).
29. J. Pouchly, and A. Zivny, *Makromol. Chem.,* **184,** 2081 (1983).
30. L. Yilmaz and A. J. McHugh, *J. Appl. Polym. Sci.,* **31,** 997 (1986).
31. P. J. Flory, *Principles of Polymer Chemistry,* Cornell University Press, 1953.
32. L. Mandelkern, in *Comprehensive Polymer Science Vol. 2: Polymer Properties,* C. Booth and C. Price, Eds., Pergamon Press, 1989, pp. 363–414.

33. J. D. Hoffman, *J. Chem. Phys.*, **28,** 1192 (1958).
34. D. W. van Krevelen, *Properties of Polymers,* Elseviers Scientific Pub. Comp., Amsterdam, 1976.
35. P. J. Flory and H. J. Daoust, *J. of Polym. Sci.*, **25,** 429 (1957).
36. P. J. A. In't Veld, P. J. Dijkstra, J. van Lochem, and J. Feijen, *Makromol. Chem.*, **191,** 1913 (1992).
37. P. van de Witte, *Thesis University of Twente,* Enschede, The Netherlands, 1994.
38. J. W. Leenslag, S. Gogolewski, and A. J. Pennings, *J. Appl. Pol. Sci.*, **39,** 2829 (1984).
39. P. van de Witte, A. Boorsma, H. Esselbrugge, P. J. Dijkstra, J. W. A. van den Berg, and J. Feijen, *Macromolecules,* **29,** 212 (1996).
40. U. Siemann, *Eur. Polym. J.*, **28,** 293 (1992).
41. *Handbook of Chemistry and Physics,* 67th ed., CRC Press, Boca Raton, FL, 1986/1987.
42. P. Triolo, *The Release of Bovine Serum Albumin from Biodegradable Poly(L-lactic acid) Matrices,* Thesis University of Utah, 1987.
43. V. P. Privalko, *J. Phys. Chem.*, **84,** 3307 (1990).
44. A. V. Lesikar, *J. Chem. Phys.*, **6,** 2297 (1975).
45. P. P. Singh and B. R. Sharma, *Z. Phys. Chemie,* **5,** 843 (1981).
46. H. C. van Ness and M. M. Abbott, *Int. Data Ser. Selec. Data Mixtures, Ser. A,* **1,** 58 (1978).
47. J. R. Goates and R. J. Sullivan, *J. Phys. Chem.*, **62,** 188 (1958).
48. C. Christensen, J. Gmehling, P. Rasmussen, and U. Weidlich, *Heats of Mixing Data Collection; Chemistry Data Series, vol. III, part I,* D. Behrens and R. Eckerman, Eds., Schön & Wertzel, Frankfurt a/M, 1984.
49. A. E. Tonelli, P. J. Flory, *Macromolecules,* **2,** 225 (1969); D. A. Brant, A. E. Tonelli, and P. J. Flory, *Macromolecules,* **2,** 228 (1969) (The values for the characteristic ratio's of PLLA and PDLLA proposed by these authors are probably too low[37]).
50. E. W. Fischer, H. J. Sterzel, and G. Wegner, *Kolloid-Z.u.Z Polymere,* **251,** 980 (1973).
51. S. Iannace, L. Ambrosio, S. J. Huang, and L. Nicolais, *J. Appl. Polym. Sci.*, **54,** 1525 (1994).
52. A. J. Nijenhuis, D. W. Grijpma, and A. J. Pennings, *Polym. Bull.*, **26,** 71 (1991).
53. R. Vasanthakumari and A. J. Pennings, *Polymer,* **24,** 175 (1983).
54. G. L. Loomis, J. R. Murdoch, and K. H. Gardner, *Polym. Preprints,* **31,** 55 (1990).
55. H. Tsuji, F. Horii, M. Nakagawa, Y. Ikada, H. Odani, and R. Kitamaru, *Macromolecules,* **25,** 4114 (1992).
56. *Polymer Handbook,* third edition, J. Brandrup and E. H. Immergut, Eds., John Wiley & Sons, New York, 1989.
57. A. Campos, R. Gavara, R. Tejero, R. C. Gomez, and B. Celda, *J. Polym. Sci.: Part B: Pol. Phys.*, **27,** 1569 (1989).
58. A. Campos, R. Gavara, R. Tejero, C. Gomez, and B. Celda, *J. Polym. Sci.: Part B: Pol. Phys.*, **27,** 1599 (1989).
59. P. Munk, M. T. Abijaoude, and M. E. Halbrook, *J. Polym. Sci.*, **16,** 105 (1978).
60. J. Pouchly and A. Zivny, *Makromol. Chem.*, **186,** 37 (1985).
61. A. Horta, D. Radic, and L. Gargallo, *Macromolecules,* **22,** 4267 (1989).
62. A. Horta, L. Gargallo, and D. Radic, *Macromolecules,* **23,** 5320 (1990).
63. J. Pouchly and A. Zivny, *Makromol. Chem.*, **184,** 2081 (1983).
64. J. B. Jackson, P. J. Flory, and R. Chiang, *Transact. Faraday Soc.*, **25,** 1906 (1963).
65. D. M. Koenhen, A. Bakker, L. Broens, J. W. A. van den Berg, and C. A. Smolders, *J. of Polymer Sci. Part B.*, **22,** 2145 (1984).
66. A. F. M. Barton, *Handbook of Polymer–Liquid Interaction Parameters and Solubility Parameters,* CRC Press, Boca Raton, FL, 1990.
67. R. Koningsveld, private communication, see also: R. Koningsveld, *Polym. Networks Blends,* **1,** 117 (1991).

Received November 9, 1995
Revised May 28, 1996
Accepted June 6, 1996